

# Development of a Predictive and Diagnostic Modeling Capability for Joule Heating

## Contents

Introduction & Background .....	5-197
Ohmic Heating of the Soil .....	5-198
The Basic Ohmic Heating Model .....	5-198
Applications of the Ohmic Heating Module .....	5-200
Conclusion.....	5-203
References.....	5-203
List of Figures .....	5-204



# **Development of a Predictive and Diagnostic Modeling Capability for Joule Heating**

**C.R. Carrigan and J.J. Nitao**

## **Introduction & Background**

The Dynamic Underground Stripping Project incorporates several remediation technologies simultaneously to mobilize and extract contaminants from both high and low permeability formations in the near-surface hydrologic regime. Understanding how steam injection into soils and ohmic heating produced by passing electrical currents through the soils interact to affect the rate of contaminant extraction has been one goal of the project. This understanding is a prerequisite to generalizing the technique for other clean-up sites. It is also necessary if the efficiency of the technique's application at a specific site is to be maximized. For the purpose of developing a predictive/diagnostic capability, we produced a generalized numerical 3-D model of the in-situ ohmic or joule heating process that has been coupled to an existing 3-D simulator for nonisothermal porous flow and transport (NUFT). This combined joule heating/hydrologic model permits a full simulation of the stripping process in a hydrologic medium of arbitrary complexity.

The ohmic heating program is modular and may either be executed with NUFT or in the standalone mode. In standalone operation, the program can be used to develop a basic understanding of how electrode placement can affect the current flow and, hence, the volumetric heating rate in a volume having a prescribed electrical conductivity distribution. In the absence of detailed hydrologic, geologic and electrochemical information, this approach may be preferred during the initial planning phases of a heating and extraction facility. The module can be used to obtain preliminary estimates of the voltage and current demands on the power supply, the localization of ohmic heating around electrodes, the effect on joule heating caused by changing electrode placement in either the horizontal or vertical coordinates as well as determining the best electrode configuration for maximizing the heating rate in specific parts of the hydrologic system. The module also simulates the application of either single phase or multiphase electrical power to the electrodes - a factor that must be considered in designing and costing an electrical system for a site.

As a module functioning interactively with the NUFT hydrologic program, a variety of complex, mutually dependent processes can be investigated. For example, the injection of steam at a well can affect the electrical conductivity through changes in both the saturation and temperature of the soil. Another phenomenon of interest is the formation of a high resistivity zone around electrodes owing to the drying out of that soil in the vicinity of the electrodes. The formation of such a zone or skin of high electrical resistivity around the electrodes will tend to redistribute ohmic dissipation so that more heating occurs locally near the electrodes rather than uniformly throughout the soil volume under consideration. Another concern that must be addressed during the operations stage is the schedule for injecting steam and for ohmic heating. Because large amounts of energy are expended to heat the soil during the stripping operation, it is desirable to determine for a particular site the most cost-effective schedule for the steam stripping/ohmic heating process.

In this report we describe our effort to develop the ohmic heating module. In addition, we will demonstrate its capability in the standalone mode and as a module of the NUFT hydrologic model.

### Ohmic Heating of the Soil

The basic problem is to model the ohmic heating produced by an arbitrary arrangement of electrodes in a volume of material that is electrically conductive. A subsidiary but important problem is to develop a model for the dependence of the electrical conductivity on the temperature, saturation and electrochemical variations of the soils and the groundwater that permeates them. This subsidiary model is necessary since conductivity is a strong function of the different soil types and saturation ranges found in a given hydrologic regime.

### The Basic Ohmic Heating Model

Figure 1 illustrates the planview of a hypothetical electrode array involving six electrodes emplaced in a volume of electrically conducting material. An alternating current (AC) power supply energizes the electrodes. The currents are phase-shifted by a designated amount at each electrode. Thus, a three phase, six electrode system might consist of electrode pairs with each pair supplied by current that was  $\pm 120^\circ$  out of phase relative to the adjacent electrode pairs. How electrode pairs are selected is

arbitrary. Electrodes in a six phase, six electrode system might be 60° out of phase with adjacent electrodes. For a uniform medium, it is found that the most uniform ohmic heating is produced by electrodes arranged on a circle and electrically phase shifted from adjacent electrodes by an amount corresponding to the angle between the electrodes as measured from the center of the circle.

The equation governing the volumes occupied by the electrodes and by the surrounding porous medium may be readily derived from the equation for charge conservation and Ohm's law. This equation may be written as:

$$\nabla \cdot \sigma \nabla \phi_s = Q_s \quad (1)$$

where  $\nabla$  is the gradient operator,  $\sigma$  is the electrical conductivity,  $\phi_s$  is the spatial electrical potential and  $Q_s$  is the spatial component of charge injected or extracted from the domain per unit volume and per unit time. In the porous medium, there is no source or sink of electrical charge, i.e.,  $Q_s=0$ . Thus, we can rewrite equation (1) as

$$\nabla \cdot \sigma \nabla \phi_s = 0 \quad (2)$$

for calculating the potential in the domain of the porous medium. The electrodes emplaced in the domain are characterized by a more or less constant conductivity  $\sigma$  and a potential  $\phi_s$  that is constant within the electrode itself. We can model the domain of the electrodes by the equations

$$\begin{aligned} \sigma &= \text{constant} \\ \phi_s &= \text{constant (at electrode)} \\ Q_s &= \text{constant (to be determined)} \end{aligned}$$

and in this regard, the electrodes may be thought of as internal boundary conditions. Implicit in this discussion is the separability of the time and spatially dependent functions  $\phi$  and  $Q$  into a spatial and a temporal part, i.e.,  $\phi = \phi_s(x,y,z)f(t)$  and  $Q = Q_s(x,y,z)f(t)$ .

The time dependence of a multi-phase electrical system is characterized by the phase shifting of each electrode potential relative to other electrodes. Recognizing that a sinusoidally varying function in time with arbitrary phase shift  $\chi$  can be written as

$$f(t) = \sin(\omega t + \chi) = \sin \omega t \cos \chi + \cos \omega t \sin \chi \quad (3)$$

permits expression of the time dependent part of each electrode potential as the sum of orthogonal sine and cosine terms. By picking the proper single value of  $\chi$  it is possible to write the time varying electrode potentials, which may be thought of as boundary conditions on the electric potential, as the sum of two orthogonal parts. Since the assigned electrode potentials tend to be different for each part of the spatial solution, it is necessary to solve for the spatial component twice. Thus, the total solution in time and space is the sum of the two orthogonal parts, i.e.,

$$\phi = \phi_{s1}(x,y,z) \cos \chi \sin \omega t + \phi_{s2}(x,y,z) \sin \chi \cos \omega t \quad (4)$$

Calculation of the change in potential across an element and the elemental values of the electrical conductivity are then used to calculate the time averaged power dissipation produced by current flow.

At this point, the module can be used to output the volumetric electrical heating or, as stated above, it can be coupled to NUFT (Nitao, 1993), the hydrologic solver, through the source term in the heat equation and also through the temperature and saturation dependence of the electrical conductivity. The dependence of the electrical conductivity on saturation, temperature and cation exchange capacity was obtained for this effort from the model of Waxman and Smits (1968).

### Applications of the Ohmic Heating Module

In the standalone mode, the Ohmic Heating Module (OHM) was employed to predict the uniformity of heating for different electrode phase relationships. The standard pattern assumed for most of the modeling was a hexagonal array of electrodes. A planview (mid-depth) for single phase heating is illustrated in Figure 2. The left and right halves of the array are maintained at different polarities. As might be anticipated, the electrodes on each side that are closest to the line of symmetry separating the left and right halves produce the greatest heating rates (lightest colors) and the electrodes farthest away produce the lowest (darkest colors). The instantaneous electric potential induced by the single phase array is also shown with positive and negative polarities indicated respectively by the light and dark coloration. Maps of the electric potential distribution are necessary for assessing the possibility of

electric shock hazards when the technique is applied to soil in occupied areas such as beneath buildings.

To date, electrode arrays have been powered by either 3-phase (LLNL) or 6-phase (PNL) power. In the case of 3-phase heating, the electrodes are paired as shown in Figure 1. Each pair is 120 degrees out of phase with its adjacent pairs. In 6-phase heating, the electrodes are each phase shifted by the same amount (60 °). The effect of 3-phase versus 6-phase power on heating uniformity is shown in Figure 3. The 6-phase array clearly produces the greatest level of uniformity in heating rate. However, 6-phase electrification of an array is somewhat more expensive to supply and like 3-phase power is not available from local utility powerlines. Furthermore, equal uniformity in the temperature distribution can be achieved with a 3-phase system if the pairings of the electrodes are switched, i.e., pairing unpaired adjacent electrodes, at suitable intervals during the time of electrification. The reason this works is that it is not the volumetric heating rate that determines the temperature distribution alone but also the length of heating time. Thus, alternating the electrode pairings on a timescale that is short compared to the characteristic thermal diffusion time scale of the target layer will achieve a temperature distribution that is comparable to the 6-phase case.

With the ohmic heating module coupled to the NUFT hydrologic simulator, a variety of heating models has been investigated. The main thrust of the modeling effort has been to investigate the effect of different electrode lengths and locations in a multilayered hydrologic model that also included the temperature, saturation and medium dependent variations in the electrical conductivity that are typically associated with layering of different soil types. The dependence of the electrical conductivity on the temperature, saturation and soil type was evaluated using the Waxman-Smits model (1968).

The electrode heating simulations were based upon the 5 layer hydrologic model illustrated in Fig. 4. This 5-layer model includes the three layers of greatest interest to dynamic stripping at the LLNL gaspad: an unsaturated, permeable sandy-clay soil called the upper steam zone (USZ), a saturated, low permeability clay layer (CON) directly beneath and another permeable, but saturated, sandy-clay layer (LSZ) beneath the clay layer. In addition, this 3-layer arrangement is bounded at the top and bottom by highly conductive and impermeable clay layers whose existence is indicated by well logs. Figure 4 also illustrates the vertical extent of the long and short electrode options that were simulated. In all simulations, the

central clay layer (CON) was the target layer for optimizing ohmic heating.

The geometrical effect of using long electrodes in this 5-layer model is illustrated in the vertical profile of volumetric heating across the five layers in Fig. 5. Assuming the same power dissipation for both long and short electrode configurations, the short electrodes in the central clay layer produce a much higher level of volumetric heating (dotted line) than do the longer electrodes (solid line). More power in the longer electrodes is lost in heating other layers and especially the top clay layer at 23 m which is penetrated by the long electrodes. For constant power levels, long electrodes are less capable of focusing ohmic heating into specific layers such as the central clay layer.

The lack of specificity in heating associated with the long electrodes is exacerbated when steam is produced at the electrodes and this steam is free to flow into the layered formation. The value of the ohmic heating technique lies mainly in its ability to heat low permeability layers that cannot be effectively flushed or heated by steam injection. Thus, when steam is produced at an electrode, two undesirable things occur. The first is that electrical energy is lost to steam that cannot effectively heat the low permeability layers. Secondly, the steam flows to other more permeable layers heating them and also enhancing their electrical conductivity so that more current flows through them. When vapor extraction from the unsaturated zone (USZ) is also taking place, the steam and, hence, the thermal energy is removed from the hydrologic system before it can even weakly influence the temperature of the central clay layer by conduction.

The 5-layer model was used to examine the effect of steam production at the long electrodes. Unlike the short electrodes used in the clay layer, the long electrodes are porous along their length and readily permit the escape of steam that is produced in the electrode wells. To model the effect of steam production on ohmic heating, a small head of steam (approx 3 psi) was maintained in the two electrode wells. The actual steam head is probably much higher so that this model is conservative in terms of the effect of steam. Figure 6 shows the temperature and volumetric heating distribution in a vertical plane intersecting the two electrodes initially and at a time 5 days into a heating simulation. The temperature plots indicate a significant increase in the temperature of the partially saturated USZ as steam has gradually flowed into this zone (note the color change between the initial and final times in the upper part of the temperature plots). The electrical conductivity has also been



modified by the flow of steam into the USZ layer. This enhances the volumetric (ohmic) heating in that layer relative to the heating in the underlying clay layer which is the target of the ohmic heating experiment. This can be seen by comparing the intensity of the color of the horizontal layer CON at the center of the plot to the intensity of the layer USZ immediately above the center. The darker layer at the earlier time becomes the brighter layer after 5 days of ohmic heating. The plot also shows a decrease in the heating rate between the clay layer at 0 days and at 5 days. In other words, less energy is being dissipated in the central clay layer after 5 days than at the start of the heating even though the total heating rate in the hydrologic system has substantially increased over the 5 day period!

### Conclusion

We have developed a predictive and diagnostic capability that can be applied to thermal remediation schemes using the ohmic heating technique. This capability has already been employed to evaluate electrode configurations in optimizing the heating of specific layers such as the central clay layer at the LLNL gaspad site. From the modeling, we have isolated several well completion and electrode design criteria that should be considered in future implementations of the ohmic heating technique.

### References

Nitao, J.J., Reference Manual for the NUFT Flow and Transport Code, Version 1.0, Lawrence Livermore National Laboratory Report, May, 1993

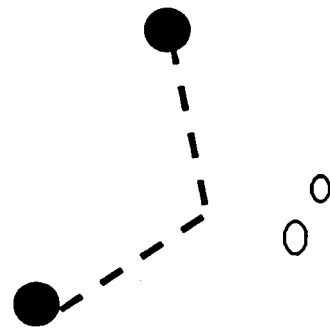
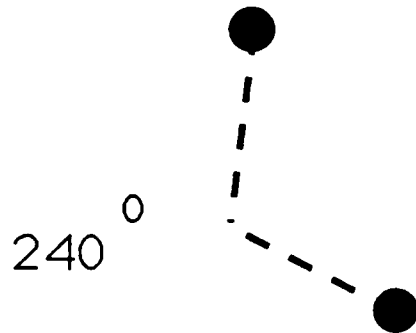
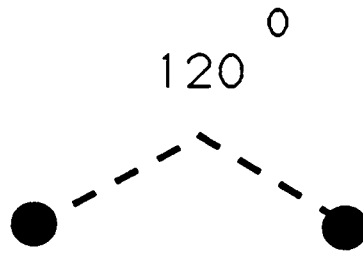
Waxman, M. and Smits, L., Electrical Conductivities in Oil-Bearing Shaly Sands, Soc. Pet. Eng. J. (1968) 107-22, Transactions, AIME, 254.

## **List of Figures**

- 1. Schematic diagram of a six-electrode array powered by 3-phase and 6-phase electrical sources.**
- 2. Planviews of the volumetric heating rate and the electric potential produced by OHM for a six-electrode array powered by a single-phase system.**
- 3. Planviews of the volumetric heating rate produced by 3- and 6-phase electrification of the electrode arrays. In the 3-phase case, the electrodes are paired as in Figure 1. Six-phase heating rates are spatially more uniform. However, 3-phase electrification with alternation of electrode pairs can produce the same level of uniformity in the temperature distribution.**
- 4. Five-layer hydrologic model assumed in OHM/NUFT simulations of the current focusing effects of long and short electrodes. The long electrodes extended across the three central layers and also penetrated the top clay layer while the short electrodes were confined to the central clay layer (CON) that was the target of the ohmic heating effort.**
- 5. Focusing effect of short electrodes is shown in plot of volumetric heating rate versus vertical coordinate (z). Power output of both long and short electrodes is held constant. At this particular location, the short electrodes are able to produce more than twice the heating rate of the long electrodes in the clay layer.**
- 6. The effect of steam production in long electrodes is simulated using the 5-layer model. Initially most of the volumetric heating, i.e., ohmic heating, is in the central clay layer where saturation is 100% (left, top). However, as steam is produced at the long electrodes, which are also porous, it flows into the permeable USZ sandy-clay zone lying above the central clay layer. This substantially increases the temperature of this zone as illustrated in the temperature plot (right, bottom). The electrical conductivity of this zone also increases with a consequential increase in the volumetric heating rate (left, bottom). It is found that volumetric heating of the clay layer decreases with time even though the total power dissipated in the hydrologic model increases over the 5-day duration of the experiment.**

# Six Electrode Planview

6 electrodes  
3 phase power



6 electrodes  
6 phase power

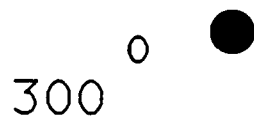
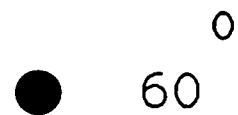
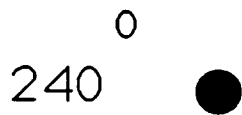
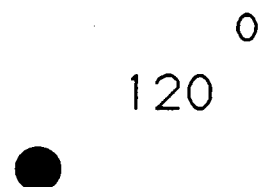
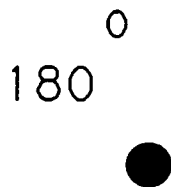
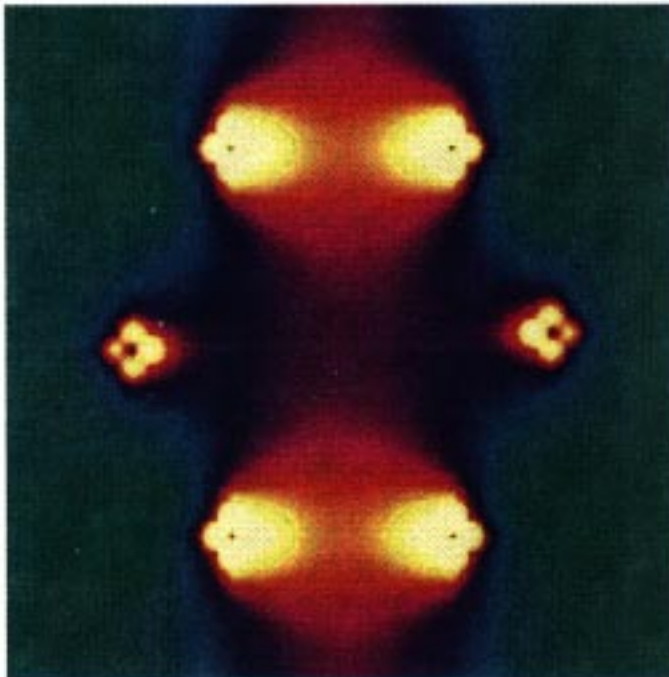


Fig. 1  
5-205



**Volumetric Heating Rate**



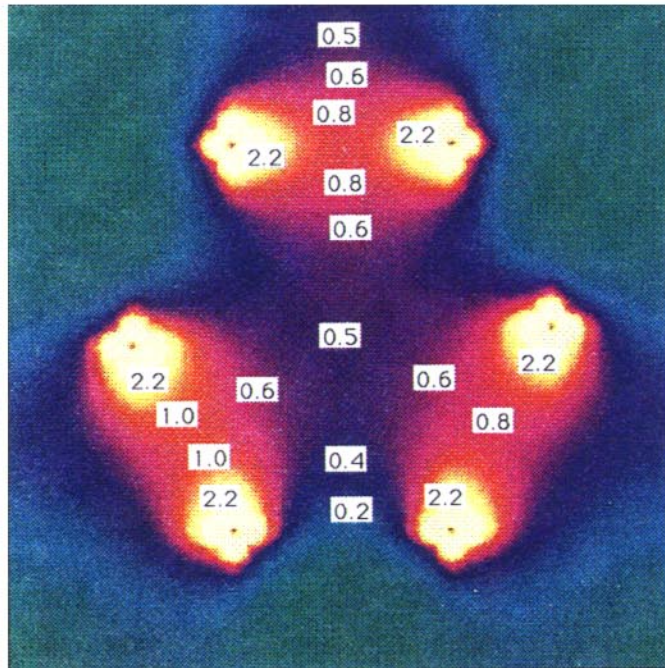
**Instantaneous Electric Field**



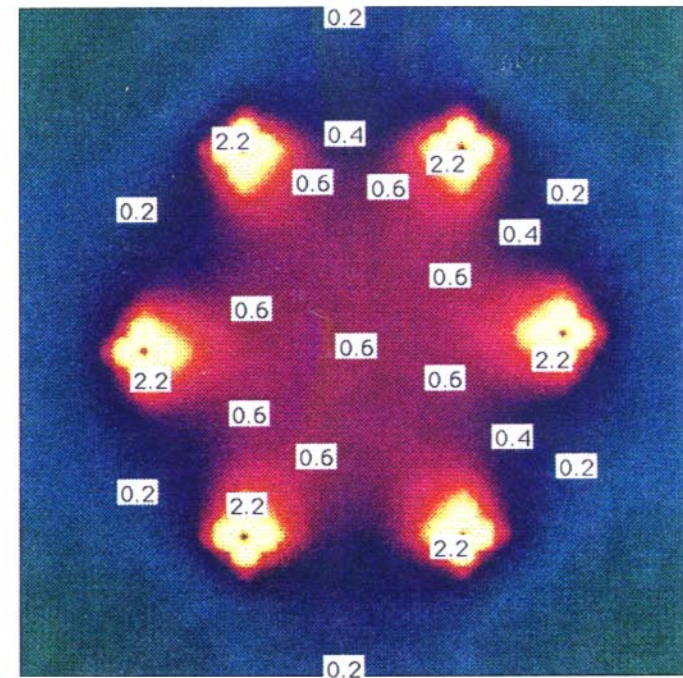
**6 Electrode / 1 Phase**

Fig. 2





**6 Electrode - 3 Phase**



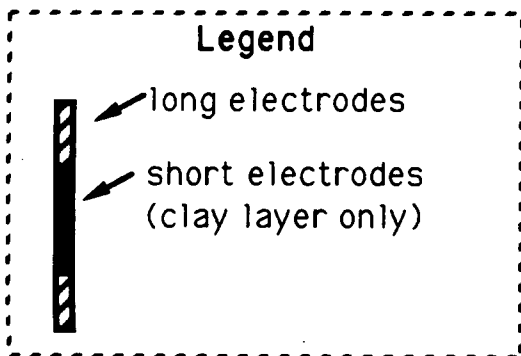
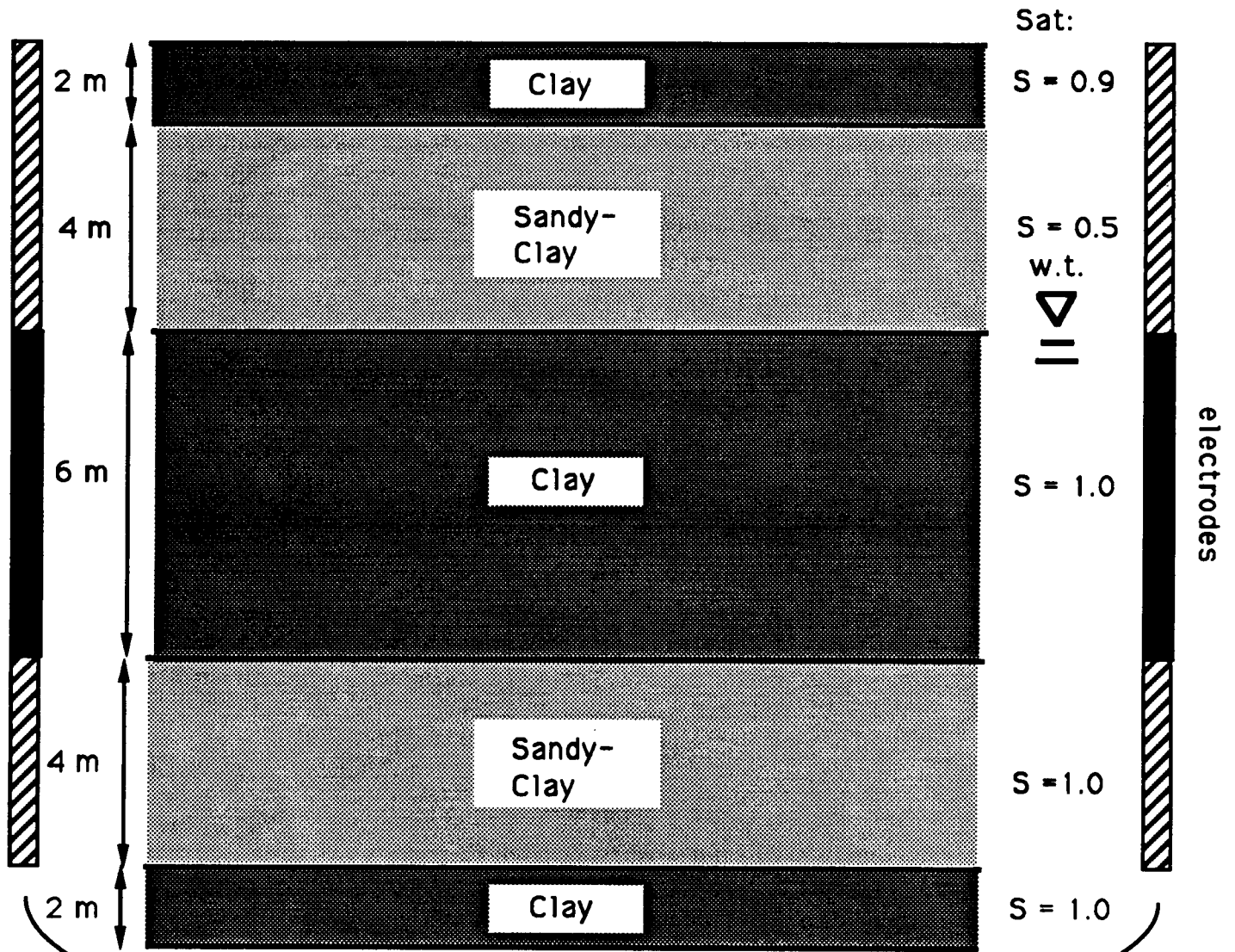
**6 Electrode - 6 Phase**

Fig. 3





## 5 - Layer Electrohydrologic Model



20 m  
electrode  
separation

Fig. 4

# Volumetric Heating

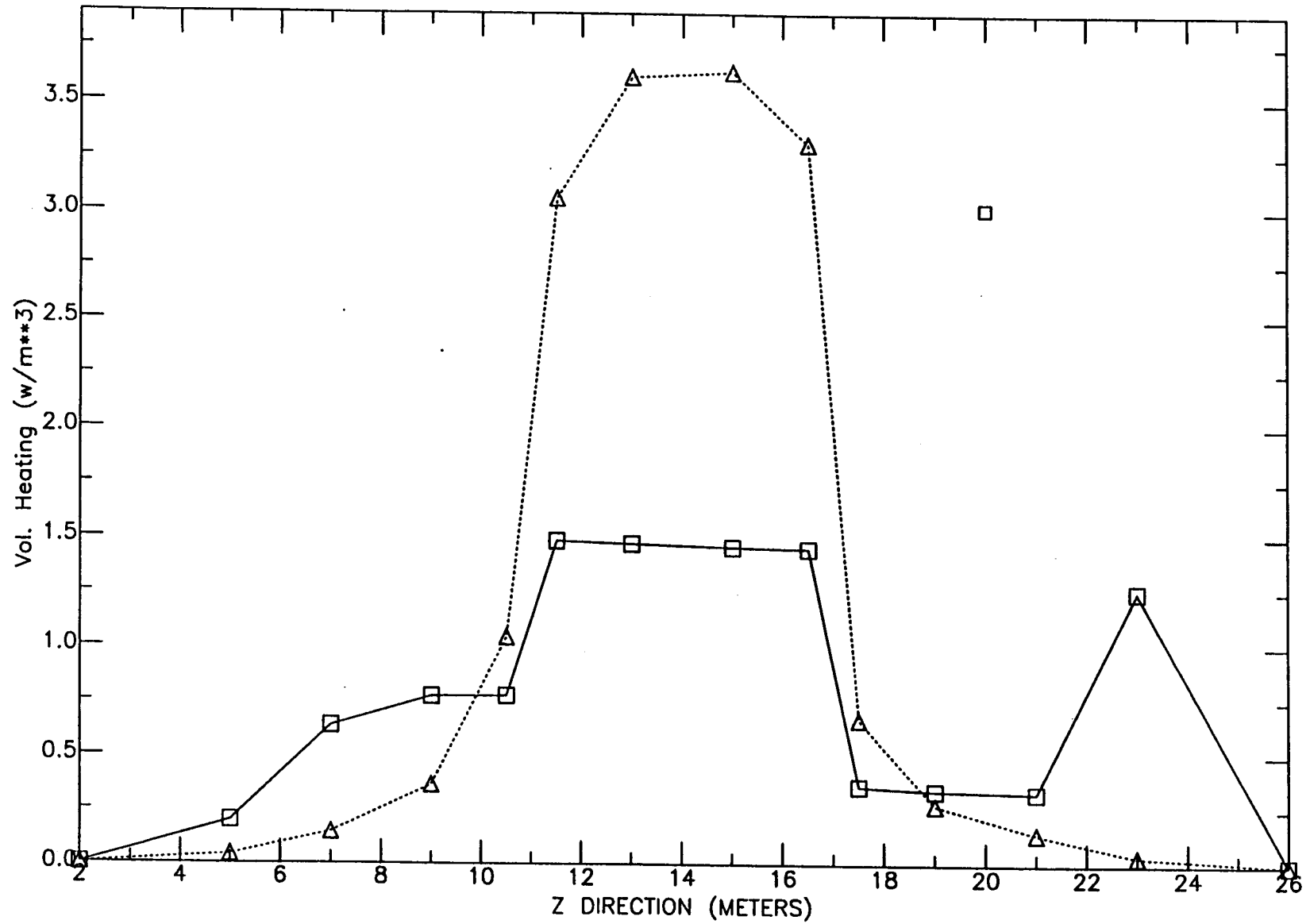
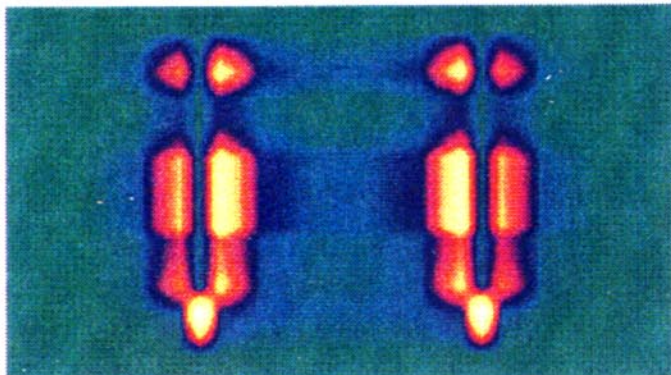


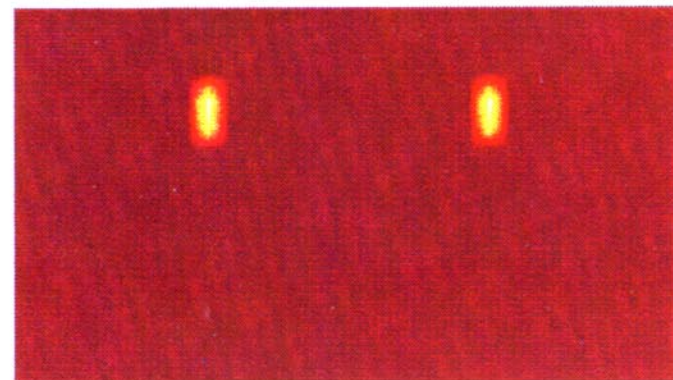
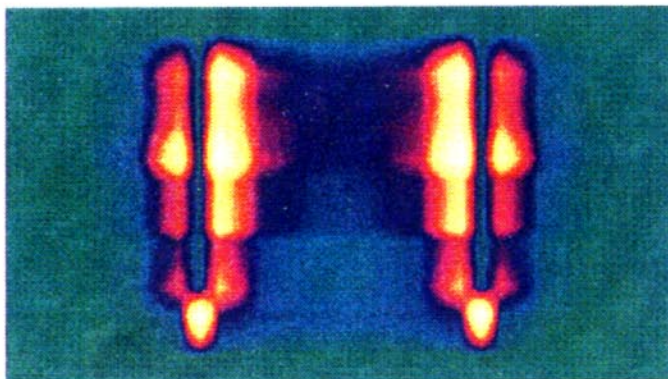
Fig. 5

**Vol. Heat Dist. - 0 Days**

USZ

con

lsz

**Temperature - 0 Days****Vol. Heat Dist. - 5 Days**

USZ

con

lsz

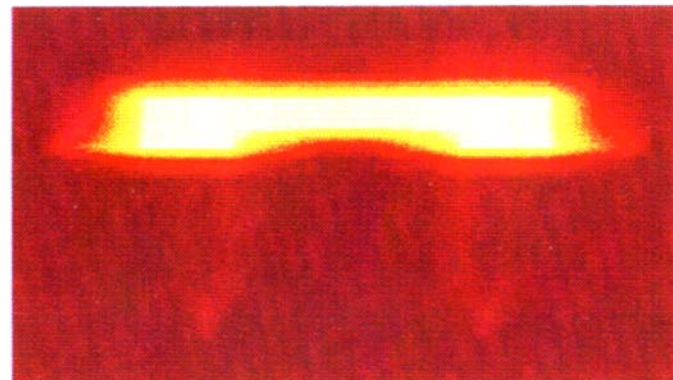
**Temperature - 5 Days**

Fig. 6



**Controlled Distribution List  
UCRL-ID-116964 Vol. 3**

**EM50**

Tom Anderson  
Dave Biancosino  
Gerald Boyd  
Clyde Frank  
Kurt Gerdes  
Joe Paladino  
Tom Parker  
Caroline Purdy  
Mac Lankford  
Steve Lien  
John Mathur  
Bill Schutte  
Jef Walker

**EM40**

Kathy Angleberger  
Paul Beam  
Tom Crandall  
John Lehr

**DOE/OK**

Mike Brown  
J. T. Davis  
Roger Liddle  
Richard Scott

**2 copies**

**US EPA TIO**

Richard Steimle

**Additional Government Copies  
Tech Partner Copies**

**20 copies  
20 copies**

**LLNL Distribution**

Roger D. Aines  
Dorothy J. Bishop  
O. Sierra Boyd  
H. Michael Buettner  
Charles R. Carrigan  
Alan B. Copeland  
William Daily  
Jay C. Davis  
Marina Jovanovich  
Paula Krauter  
Thomas J. Kulp  
Kevin C. Langry  
Kenrick H. Lee

James Martin  
Roger E. Martinelli  
J. C. Nelson-Lee  
Robin L. Newmark  
Abelardo L. Ramirez  
Maureen N. Ridley  
William H. Siegel  
Jerry J. Sweeney  
Bruce Tarter  
Lee Younker  
Jesse Yow (4 copies)  
John Ziagos

**Weiss Associates, Inc.,**  
**Emeryville, CA**  
Charles Noyes  
Everett A. Sorensen

**Infraseismic Systems Inc.,**  
**Bakersfield, CA**  
Roger J. Hunter

**Department of Mechanical Engineering,**  
**University of California,**  
**Berkeley, CA**  
Ron Goldman  
Kent M. Kenneally  
Kent S. Udell

**Health Sciences Research Division,**  
**Oak Ridge National Laboratory,**  
**Oak Ridge, TN**  
Tye E. Barber  
Eric A. Wachter

**Materials Science and Minerals Engineering**  
**Department,**  
**University of California,**  
**Berkeley, CA**  
A. E. Adenekan  
T. W. Patzek